FRCM confinement as a repair technique for seismically damaged RC columns

Klajdi Toska[1*], Lorenzo Hofer[1], Flora Faleschini[1,2], Mariano Angelo Zanini[1], Carlo Pellegrino[1]

1. Department of Civil, Environmental and Architectural Engineering, University of Padova, Via Marzolo 9, 35131 Padova, Italy.
2. Department of Industrial Engineering, University of Padova, Via Gradenigo 6, 35131 Padova, Italy

[*]Corresponding author email: klajdi.toska@dicea.unipd.it

Abstract

The research work deals with the experimental behavior of undamaged reinforced concrete (RC) columns and seismically-damaged repaired RC columns under increasing cyclic lateral loading. Two real-scale elements were initially tested under constant axial and increasing cyclic lateral loading to simulate a seismic damage. A repair protocol, designed to restore the initial strength of the elements, was then followed. Based on the initial damage observed on the specimens, two repair methods were adopted: for damage concentrated only in the concrete, column base was confined through fabric reinforced cementitious mortar (FRCM), while, for damage also extended to the bending steel reinforcement, additional FRCM flexural reinforcement was embedded in the confinement jacket. Results of undamaged and repaired specimens are presented and compared in terms of cracking pattern, load-displacement curves, ductility, stiffness degradation and energy dissipation. During the loading history, fiber strains were monitored in the repaired columns through electrical strain gages previously installed in the fabric. The experimental results show that FRCM composites can be effectively used to restore strength and ductility of RC columns previously damaged by cyclic lateral loading.

1 INTRODUCTION

Externally bonded reinforcement systems have been widely used in the last decades to strengthen and repair existing RC and masonry structures. Traditional FRP (fiber reinforced polymer) composites and the more recent FRCM or TRM (textile reinforced mortar) composites have been proved to significantly improve strength and ductility of retrofitted elements. Among others, confinement is one of the main interventions to enhance seismic behavior where the above composites are adopted.

While extensive experimental campaigns, even on real-scale elements, have been carried out in the last decades to investigate FRP confinement effectiveness as a seismic retrofitting technique [1-3], literature investigating seismic behavior of real-scale FRCM confined RC columns is still very limited. FRCM confinement is believed to be less effective than the FRP one according to some recent studies [4-6]. Some of the authors investigated the effectiveness of FRCM confinement to repair RC columns previ-

ously damaged due to excessive axial loading [7]. Different cross-sections and internal steel reinforcement configuration were considered and results showed that FRCM confinement was able to enhance significantly the residual strength of the damaged elements. While, as expected, circular cross-section columns performed better than the square ones. In [8] Toska and Faleschini investigated the behavior of FRCM confined concrete under axial cyclic loading. The experimental results showed that the stress-strain behavior highly depend on the number of layers applied, fiber material and on the cross-section shape of the specimens. Regarding the seismic behavior of repaired RC columns it is worth mentioning the experimental campaign carried out by Saadatmanesh et al. [9] to evaluate the FRP confinement effectiveness to adequately repair RC columns damaged under lateral cyclic loading. More recently, Feng et al. [10] investigated the seismic behavior of RC columns affected by corrosion and strengthened through Carbon FRCM confinement. According to the results corroded specimens showed a significant reduction in terms of secant stiffness, strength, ductility and energy dissipation capacity with respect to the uncorroded ones and confinement through carbon FRCM confinement was able to enhance all previously mentioned parameters in retrofitted corroded RC columns.

The goal of the presented experimental work is to investigate the effectiveness of FRCM confinement to repair earthquake damaged RC columns. two real-scale control specimens were initially tested applying both a constant axial and a fully-reversed increasing cyclic lateral displacement at column top. Control specimens were then repaired through FRCM composites using two different strengthening schemes, and tested under the same loading protocol.

2 EXPERIMENTAL CAMPAIGN

The experimental campaign presented in this paper consists in four lateral cyclic loading tests. Initially, a significant seismic damage was induced in two real-scale RC columns by cyclic lateral loading. Subsequently, the damaged specimens were repaired through FRCM composites and subjected to the same test as the original ones.

2.1 Materials and specimens

Specimens are characterized by a square section with side b = 400 mm and height of 2900 mm and were casted over a foundation block of 1400 x 1800 mm which was designed to remain elastic during the loading history. Two internal steel reinforcement configurations are adopted. The first specimen (P30) is reinforced with four diameter 30 mm bars placed at the corners of the section and four diameter 12 mm bars placed in the middle of each side. In the second one (P24) main reinforcement consists of four diameter 24 mm bars while the four bars in the middle of each section side remain the same ($d = 12\ mm$). Stirrups with 100 mm of spacing and 10 mm of diameter are adopted in both specimens as shows in Figure 1. Columns were designed following the provisions of NTC18 [11], EC2 [12] and EC8 [13] for medium ductility class elements. Reinforcement steel properties are shown in Table 1 in terms of yield strength (f_y), ultimate strength (f_t), and respective strains (ε_y and ε_t). The values reported in Table 1 are the mean of experimental tensile tests carried out on three specimens for each diameter considered. Columns were casted separately and the concrete properties are shown in Table 2 for each column as mean values of three tested samples for each parameter.

Table 1. Steel properties for each reinforcement bar.

Diameter	f_y [MPa]	ε_y [%]	f_t [MPa]	ε_t [%]
30	*572*	*0.27*	*673*	*19.8*
24	*537*	*0.26*	*648*	*17.4*
10	*526*	*0.26*	*623*	*12.0*

Table 2. Concrete mechanical properties.

Specimens	f_c [MPa]	E_c [MPa]
P30	*45*	*36700*
P24	*50*	*39800*

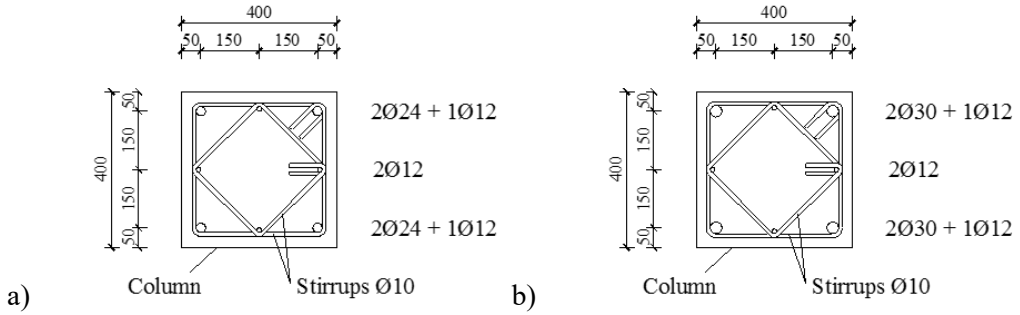

Figure 1. Column reinforcement a) P24 and b) P30 specimens.

The original columns were tested under the same setup and loading protocol detailed in Hofer et al. [14]. Load was applied under a displacement control mode and for each lateral displacement increment, three full cycles were applied at the top of the column. During the lateral loading history, the vertical load was maintained constant (300 kN for P30 and 350 kN for P24 specimens) using an actuator placed at the top of the column and anchored at the column foundation using two steel bars. Steel bars were hinged at the foundation in order to avoid any *P-Δ* effects during the test. Figure 3b shows a frame of the specimens during testing.

After the original, undamaged columns were tested, damage inspection was carried out. Both specimens showed significant visible damage at the column base where large crack opened and concrete cover was lost. The observed damage was higher in the P24 column where one diameter 12 mm bar failed while the main bars showed some slight buckling phenomena. UPV (ultrasonic pulse velocity) was used to map the damage in the tested specimens. The propagation velocity of the ultrasonic waves was measured using the direct method and then the concrete dynamic elastic moduli (E_d) was computed following equation 1.

$$E_d = \frac{{v_p}^2 \cdot \rho \cdot (1+\nu) \cdot (1-2\nu)}{(1-\nu)} \qquad (1)$$

The results of the UPV tests are shown in Figure 2. At the column base, where damage was concentrated and concrete cover was lost, it was not possible to measure the wave propagation velocity.

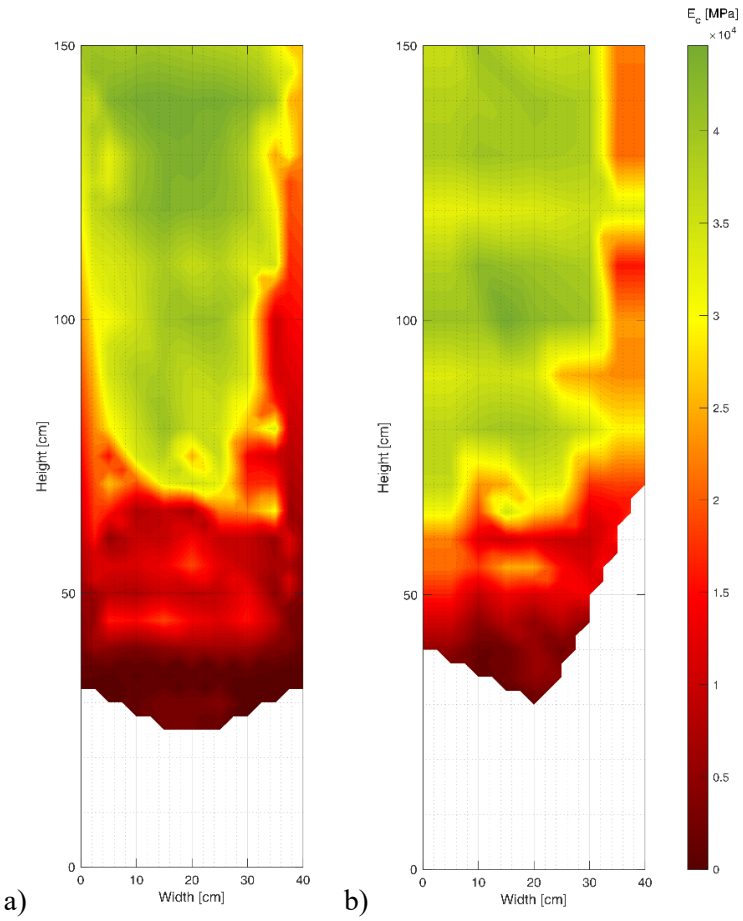

Figure 2. UPV test results for (a) P30; and (b) P24 columns.

2.2 FRCM repair intervention

After testing, damaged specimens were prepared for the repair interventions. First, detached concrete fragments were removed and the columns surfaces were cleaned. Base section of the columns, where the cover was lost, was restored to the initial geometry using the same mortar adopted for the FRCM system. Following the Italian guidelines for the design of fiber reinforced cementitious composites [15] recommendations, the corners of the square section were rounded (40 mm radius) before the confinement application to limit stress concentration and local fiber failure in the corners. Figure 3a shows specimens P24 during confinement application.

The first meter of the columns base was confined using two carbon fabric layers applied by alternating mortar (about 4-5 mm thick) and fabric layers. Carbon fabric was applied continuously with an overlapping length of 400 mm, as recommended by [15]. In the P24 specimens, due to the high damage observed after the first test, additional bending moment FRCM reinforcement was embedded in the confinement jacket, in order to restore the initial lateral strength of the element. The flexural reinforcement consists of 122 mm^2 of carbon fibers applied in both sides of the column. Mechanical prop-

erties for mortar, determined on at least three 40 x 40 x 160 mm prismatic specimens following standard EN 1015–11 [16], are reported in Table 3 in terms of flexural strength (f_f) and compressive strength (f_c). Regarding carbon fibers, its experimental properties were obtained through tensile tests on at least five specimens and are shown in Table 4.

Table 3: FRCM mortar mechanical properties

Specimen ID	f_f [MPa]	*Std Dev* [MPa]	f_c [MPa]	*Std Dev* [MPa]
P24	5.17	0.46	51.20	7.04
P30	6.71	0.62	41.65	7.12

Table 4: FRCM carbon fiber mechanical properties

Type	Material	t_f [mm]	f_{fu} [MPa]	ε_{fu} [%]	E_f [MPa]
Experimental	Carbon	0.61	1315	0.89	206400

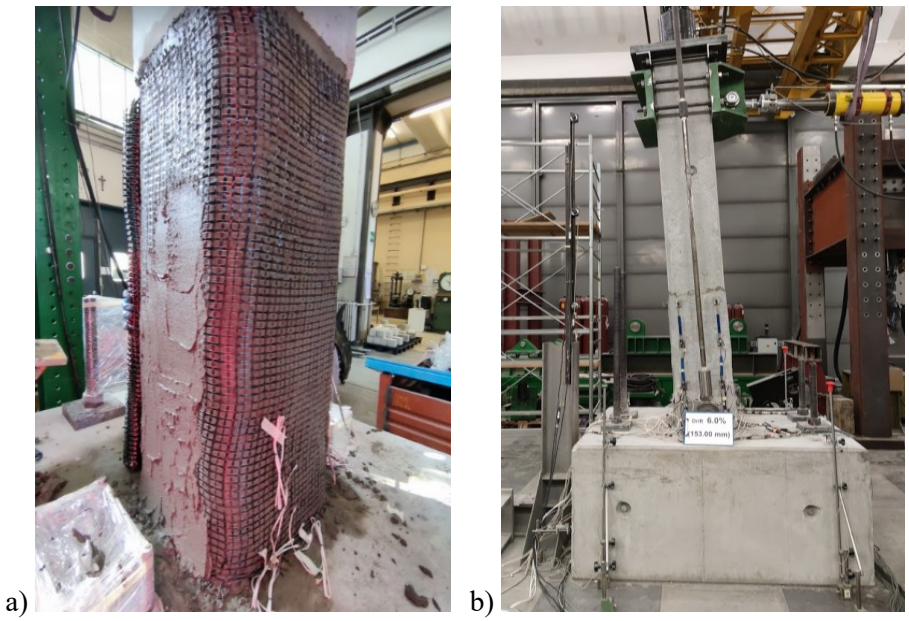

a) b)

Figure 3: a) FRCM confinement application, b) specimen during lateral cyclic testing.

3 EXPERIMENTAL RESULTS

3.1 Crack pattern

During the test, cracks that gradually formed in the faces of the columns were marked with the use of plaster. To associate each crack with a specific drift level, different colors were used. The distribution of these cracks in the faces is visible in Figure 19 for the P30 column. The faces being perpendicular to the direction of application of the load are here-in called " Front " and " Back ', while the lateral ones' Side A 'and' Side B '. The distribution of these cracks in the faces is visible in Figure 4 for the P30 column.

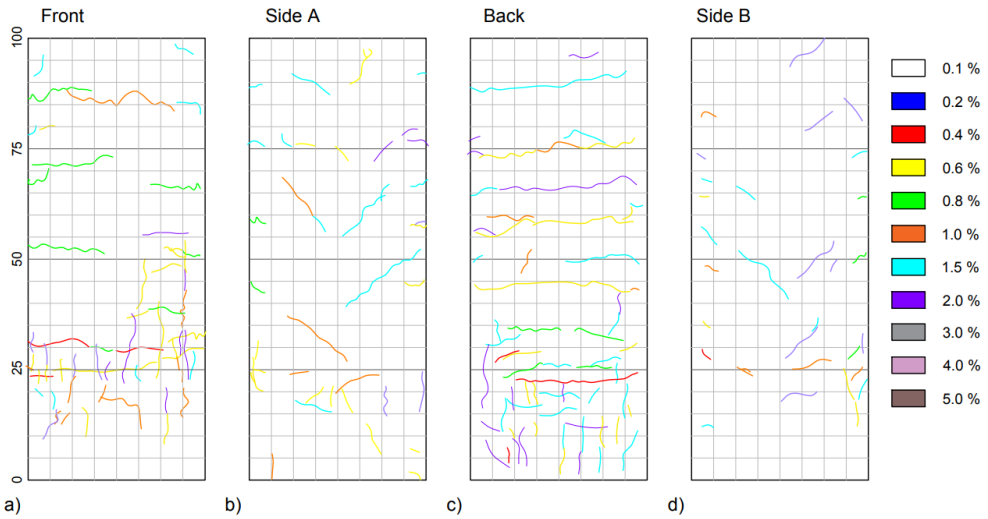

Figure 4: Crack distribution for the P30 specimen confined through FRCM.

The observed cracks were generally more concentrated, for both columns, in the faces orthogonal to the direction of the horizontal load being in this case horizontal. For the lateral faces crack are less diffused, start to appear later in the loading history and they mainly develop along the diagonal direction.

Apart from the diffused cracking patter, the confined P30 column maintained its integrity throughout the loading history without recording significant strength degradation. On the other hand, on the confined P24 column significant damage was observed during the last loading cycles which also led to a significant reduction of the load-bearing capacity, even though the overall reduction was not higher than that observed in the undamaged specimen. After the test, damage inspection found out that one main bar per side (diameter 24 mm) had failed and significant damage was also observed on the FRCM flexural reinforcement with some localized fiber failure on both sides. Figure 5 and 6 show respectively the main bar failure and FRCM bending reinforcement failure observed in the P24 column.

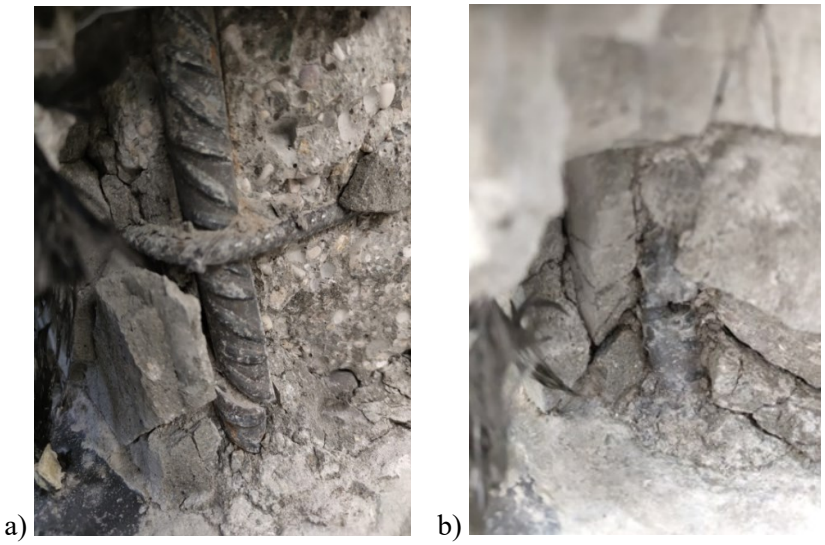

Figure 5: a) and b) main reinforcement bar failure (P24).

a)  b) 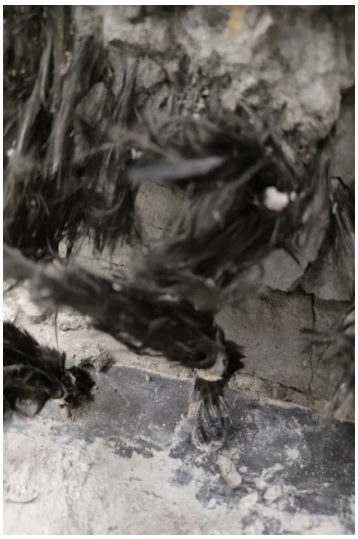

Figure 6:Carbon fiber flexural reinforcement failure (P24).

3.2 Load vs top displacement

Hysteretic responses are shown in Figure 7 a) for P30 columns and b) for P24 ones. In the first case, very similar behavior between undamaged and repaired specimens both in terms of peak-load and ductility was observed. Worth mentioning that for P30 columns no significant damage was observed until 5% drift ratio (only 10% strength reduction) was reached and due to laboratory limits the columns could not be pushed beyond that limit. Both undamaged and repaired elements display almost a symmetric behavior during the push-pull cycles with the peak load being slightly higher in the pull conditions. The main difference between the two elements behavior is observed in the first almost linear branch with the damaged specimen showing an initial stiffness much lower than that of the undamaged one. This is because in the case of the P30 column the repair intervention concerned only the confinement of the column and no additional flexural reinforcement was added. Also, cracks opened from the first test were not sealed by means of injections neither in the P30 nor in the P24 columns, limiting the intervention to the restoration of the most damaged section at the base with normal mortar. The lower initial stiffness determines also a higher drift value at the yielding point with respect to the undamaged conditions.

a) 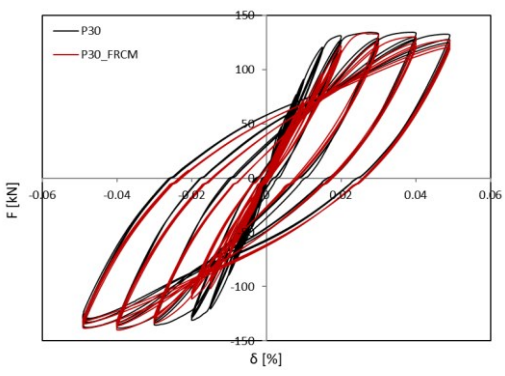

b) 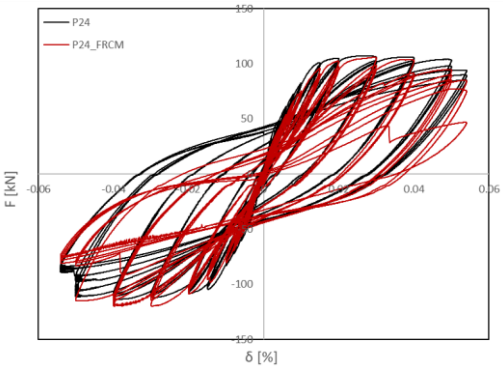

Figure 7: Comparison of Force (F) vs drift ratio (δ) curves between undamaged and repaired elements for P30 (a) and P24 (b)

It is worth recalling that, for the P24 column, due to the high damage observed in the longitudinal steel reinforcement after the first test on the undamaged element, additional flexural reinforcement, designed to restore initial strength, was added through the same FRCM system. Considering the initial severely-damaged conditions, where a 30% load reduction was recorded in the first test, very promising results were obtained through the FRCM repair protocol. Peak load was almost equaled in push cycles (106 kN for P24_FRCM and 107 kN for P24) while for pull cycles peak load of the repaired element resulted even higher than the one recorded on the undamaged one (120 vs 113 kN). Similar ductility was observed in both elements even though a higher strength degradation was observed in the repair element for repeated cycles at the same drift level. Finally, unlike the P30 columns, for the P24 ones similar initial stiffness was observed for both undamaged and repaired specimens. Since FRCM confinement is ineffective to enhance both axial and lateral stiffness of retrofitted elements as the experimental evidence, provided in the previous sections shows, this is mainly due to the additional flexural reinforcement applied through Carbon-FRCM.

3.3 Energy dissipation

When dealing with seismic actions the ability of the structures to dissipate energy is a very important factor in the overall seismic behavior. The dissipated energy can be computed for each cycle as:

$$E_{d,i} = \oint F(\Delta) d\Delta \qquad (2)$$

while the cumulative energy dissipated during the loading history is:

$$\sum E_{d,i} = \sum_i^n E_{d,i} \qquad (3)$$

The results for both cycle dissipated energy ($E_{d,i}$) and cumulative dissipated energy ($\sum E_{d,i}$) are shown in Figure 8 for P30 columns and Figure 9 for P24 ones. The dissipated energy is very similar for undamaged and for repaired elements both comparing single cycle values and the cumulative energy. The cumulative energy results slightly lower in the case of repaired specimens but the difference is small enough to be considered negligible.

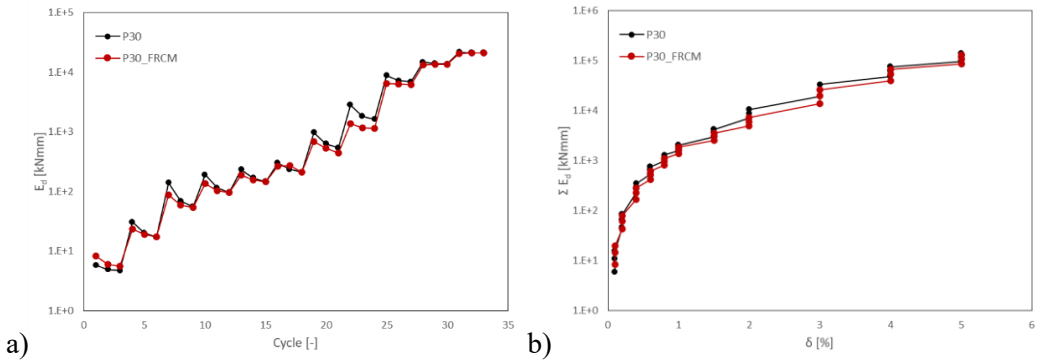

Figure 8: Dissipated energy for each loading cycle (a), and cumulative dissipated energy (b) for the P30 specimens

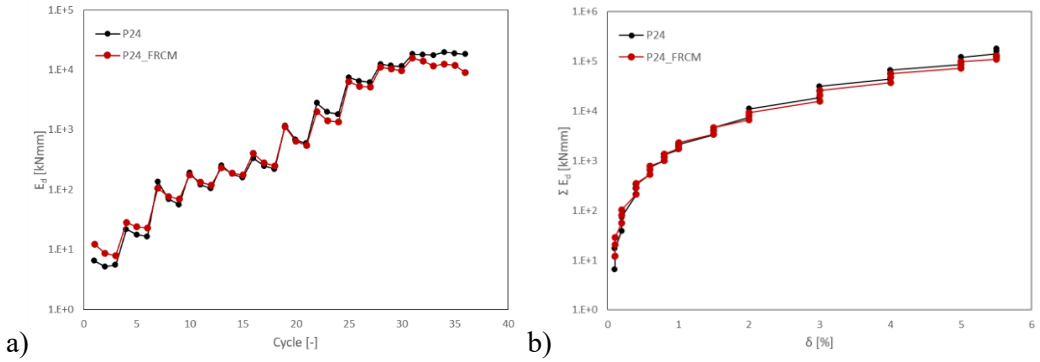

Figure 9: Dissipated energy for each loading cycle (a), and cumulative dissipated energy (b) for the P24 specimens

3.4 Stiffness degradation

The secant stiffness degradation K_i is defined as the ratio of the lateral load to the corresponding displacement:

$$K_i = \frac{|\pm F_i|}{|\pm \Delta_i|} \tag{4}$$

where K_i is the secant modulus at the i-*th* drift level, F_i and Δ_i are the peak load of the hysteretic loop and corresponding displacement at the i-t*h* drift level.

Figure 10 shows the degradation of the secant stiffness for P30 and P24 columns, for both control (black color) and repaired (red color), at increasing drift values. Continues line identifies the push loading direction, whereas dashed line the pull one. The P24 columns have a slightly higher elastic stiffness than P30, because it is subject to a higher axial loading, and the concrete batch used has a slightly higher elastic modulus. Stiffness degradation curves are almost overlapping for the push and pull cycles for all the specimens. The two different strengthening schemes for the two specimens have a different influence on the column stiffness. Regarding the first loading cycles, the presence of flexural reinforcement provided by the anchored carbon bending reinforcement in the P24_FRCM specimen was able to restore the 86% of the initial stiffness of the undamaged column. Instead, the confinement provided by the fibers in the P30_FRCM specimen allowed to reach only the 73% of initial stiffness of the original P30 column. For both P30_FRCM and P24_FRCM specimens, the stiffness at the last loading cycles starting from δ = 2÷3%, is very close to that of the control columns.

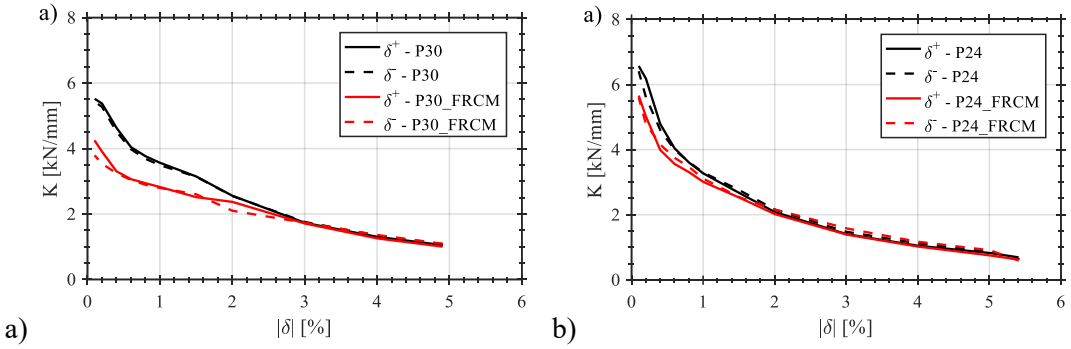

Figure 10. Secant stiffness deterioration of control and repaired P30 a) and P24 b) columns.

4 CONCLUSIONS

The effectiveness of FRCM confinement to adequately repair seismically damaged RC columns was investigated in this experimental activity. Full-scale elements were initially damaged under cyclic lateral loading then repaired through FRCM confinement and finally re-tested following the same loading protocol. According to the experimental results obtained the following conclusions can be drawn:

- FRCM confinement can restore strength and lateral displacement capacity on seismically damaged RC elements;
- Additional FRCM bending reinforcement can be embedded in the FRCM confinement jacket enhancing strength and restoring the initial stiffness of severely damaged columns;
- The repaired RC columns dissipate almost the same energy with respect to the original undamaged ones;
- Initial secant stiffness of repaired elements results lower compared to the control specimens. Repair intervention including FRCM bending reinforcement allows a significant recover of the initial stiffness compared to only confinement.

REFERENCES

[1] Lim, J. C., & Ozbakkaloglu, T. (2015). Hoop strains in FRP-confined concrete columns: experimental observations. Materials and Structures, 48(9), 2839-2854.

[2] Rousakis, T. C., Karabinis, A. I., & Kiousis, P. D. (2007). FRP-confined concrete members: Axial compression experiments and plasticity modelling. Engineering Structures, 29(7), 1343-1353.

[3] Realfonzo, R., Napoli, A., & Pinilla, J. G. R. (2014). Cyclic behavior of RC beam-column joints strengthened with FRP systems. Construction and Building Materials, 54, 282-297.

[4] Donnini, J., Spagnuolo, S., & Corinaldesi, V. (2019). A comparison between the use of FRP, FRCM and HPM for concrete confinement. Composites Part B: Engineering, 160, 586-594.

[5] Fossetti, M., Alotta, G., Basone, F., & Macaluso, G. (2017). Simplified analytical models for compressed concrete columns confined by FRP and FRCM system. Materials and Structures, 50(6), 1-20.

[6] Triantafillou, T. C., & Papanicolaou, C. G. (2005). Textile Reinforced Mortars (TRM) versus Fiber Reinforced Polymers (FRP) as Strengthening Materials of Concrete Structures. Special Publication, 230, 99-118.

[7] Toska, K., Faleschini, F., Zanini, M. A., Hofer, L., & Pellegrino, C. (2021). Repair of severely damaged RC columns through FRCM composites. Construction and Building Materials, 273, 121739.

[8] Toska, K., & Faleschini, F. (2021). FRCM-confined concrete: Monotonic vs. Cyclic axial loading. Composite Structures, 268, 113931.

[9] Saadatmanesh, H., Ehsani, M. R., & Jin, L. (1997). Repair of earthquake-damaged RC columns with FRP wraps. ACI Structural Journal, 94, 206-215.

[10] Feng, R., Li, Y., Zhu, J. H., & Xing, F. (2021). Behavior of corroded circular RC columns strengthened by C-FRCM under cyclic loading. Engineering Structures, 226, 111311.

[11] Norme Tecniche per le Costruzioni (2018). Ministerial Decree 17/01/2018. In Italian

[12] EC2 (EN 1992) (2014) Eurocode 2: Design of concrete structures.

[13] EC8 (EN 1998) (2014) Eurocode 8: Design provisions for earthquake resistance of structures.

[14] Hofer, L., Zanini, M. A., Faleschini, F., Toska, K., & Pellegrino, C. (2021). Seismic behavior of precast reinforced concrete column-to-foundation grouted duct connections. Bulletin of Earthquake Engineering, 19(12), 5191-5218.

[15] Consiglio Nazionale delle Ricerche, CNR DT 215-2018. Istruzioni per la Progettazione, l'Esecuzione ed il Controllo di Interventi di Consolidamento Statico mediante l'utilizzo di Compositi Fibrorinforzati a Matrice Inorganica, 2018 (in Italian).

[16] EN 1015-11:1999/A1:2006. Methods of test for mortar for masonry - Part 11: Determination of flexural and compressive strength of hardened mortar. Brussels, Belgium: CEN; 2006.
[17] ACI 374.1-05 (2014) Acceptance criteria for moment frames based on structural testing and commentary.